Slipped-cofacial J-type phthalocyanine dimers as potential non-linear absorbers for optical limiting applications

Alexander Yu. Tolbin,[a] Alexander V. Dzuban,[b] Evgeny V. Shulishov,[c] Larisa G. Tomilova[a,b] and Nikolay S. Zefirov[a,b]

[a] Institute of Physiologically Active Compounds, Russian Academy of Sciences, 142432 Chernogolovka, Moscow Region (Russian Federation)
[b] Department of Chemistry M. V. Lomonosov Moscow State University, 119991 Moscow (Russian Federation)
[c] N.D. Zelinsky Institute of Organic Chemistry (ZIOC RAS), 119991 Moscow, Russian Federation

* Corresponding author. Tel.: +7 496 5242566, e-mail address: tolbin@ipac.ac.ru (Prof. A.Yu. Tolbin).

TABLE OF CONTENTS

1. MALDI-TOF mass spectra

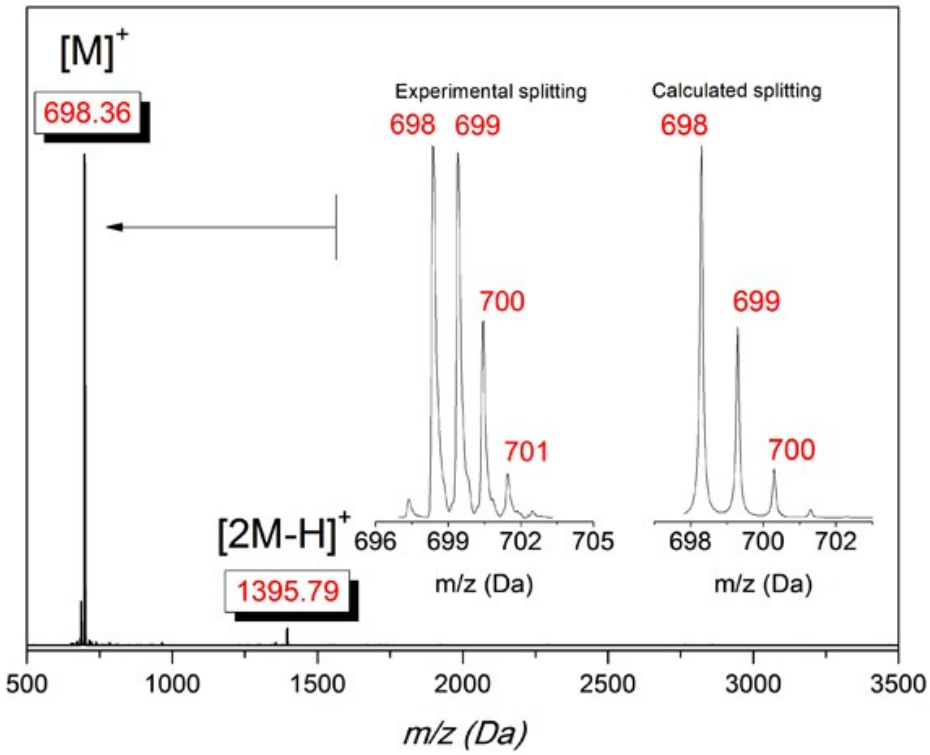

Fig. S1. MALDI-TOF mass spectrum of Compound **1**.

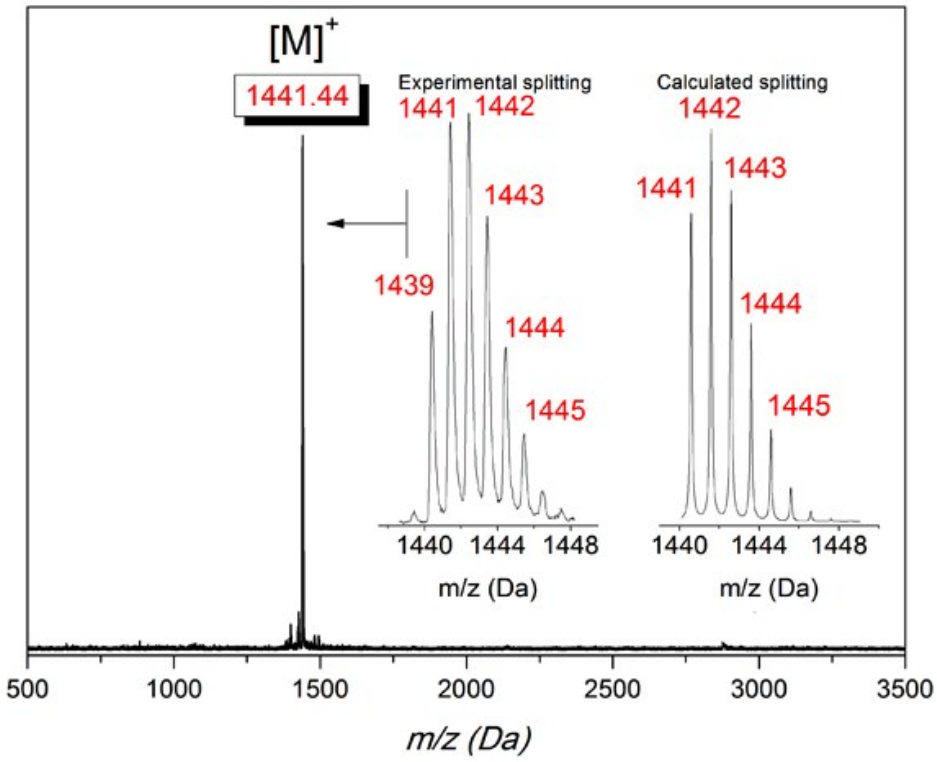

Fig. S2. MALDI-TOF mass spectrum of Compound **2**.

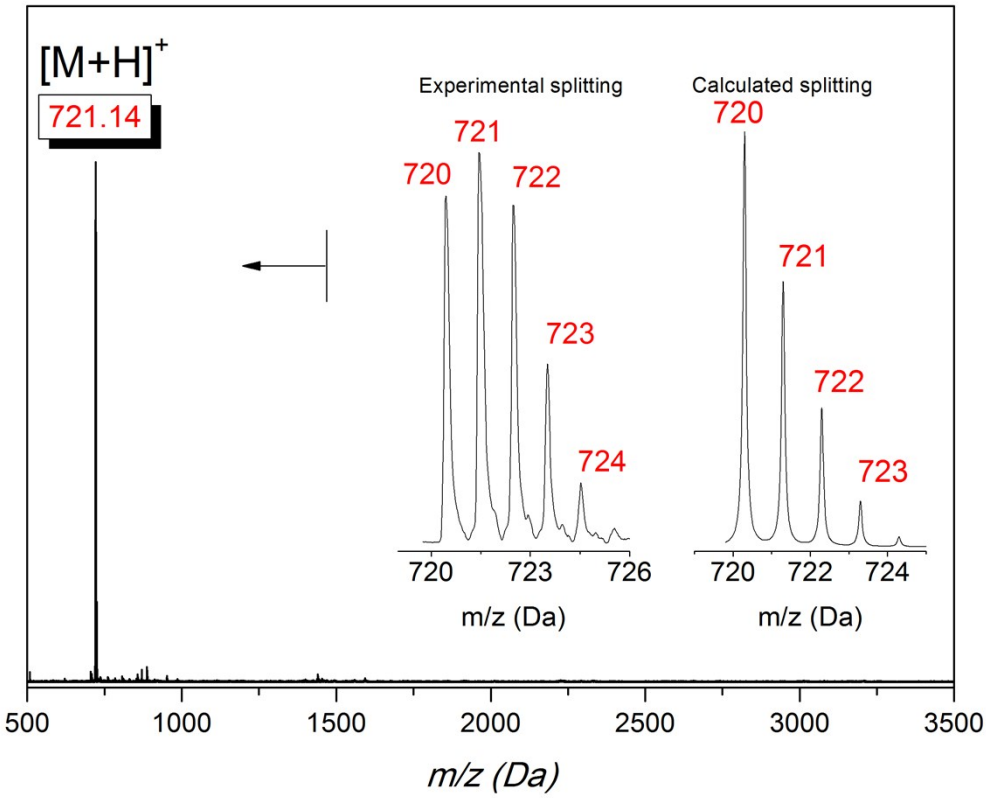

Fig. S3. MALDI-TOF mass spectrum of Compound **3**.

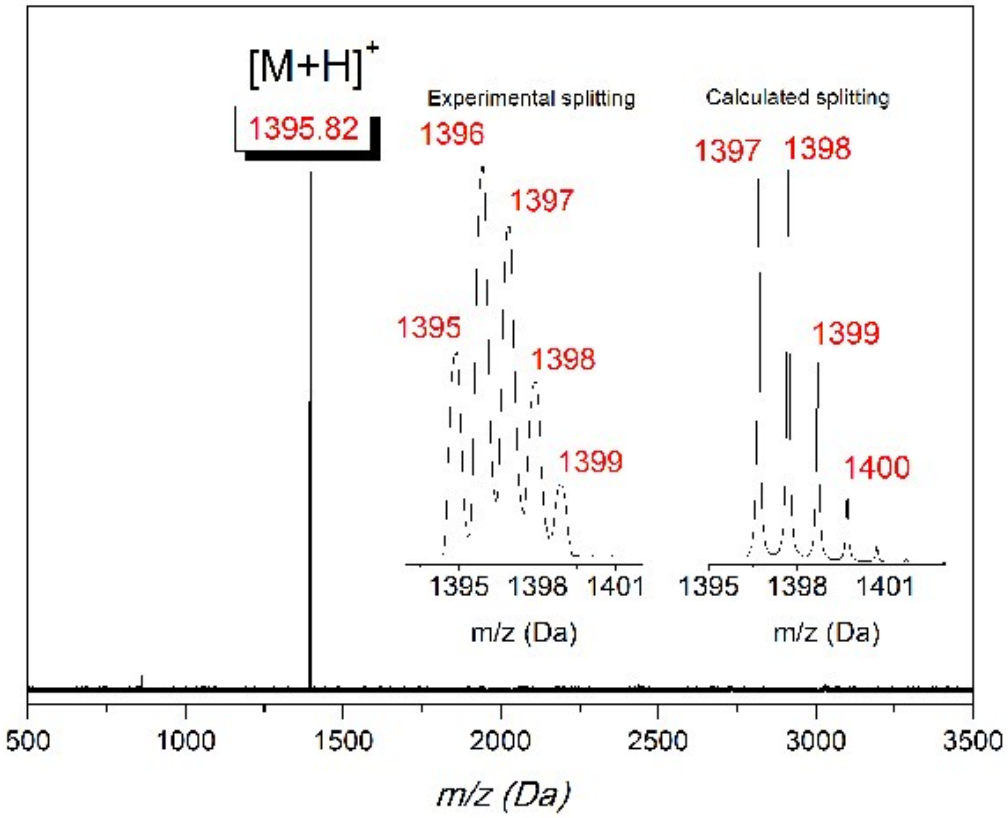

Fig. S4. MALDI-TOF mass spectrum of Compound **4**.

2. Proton NMR spectra

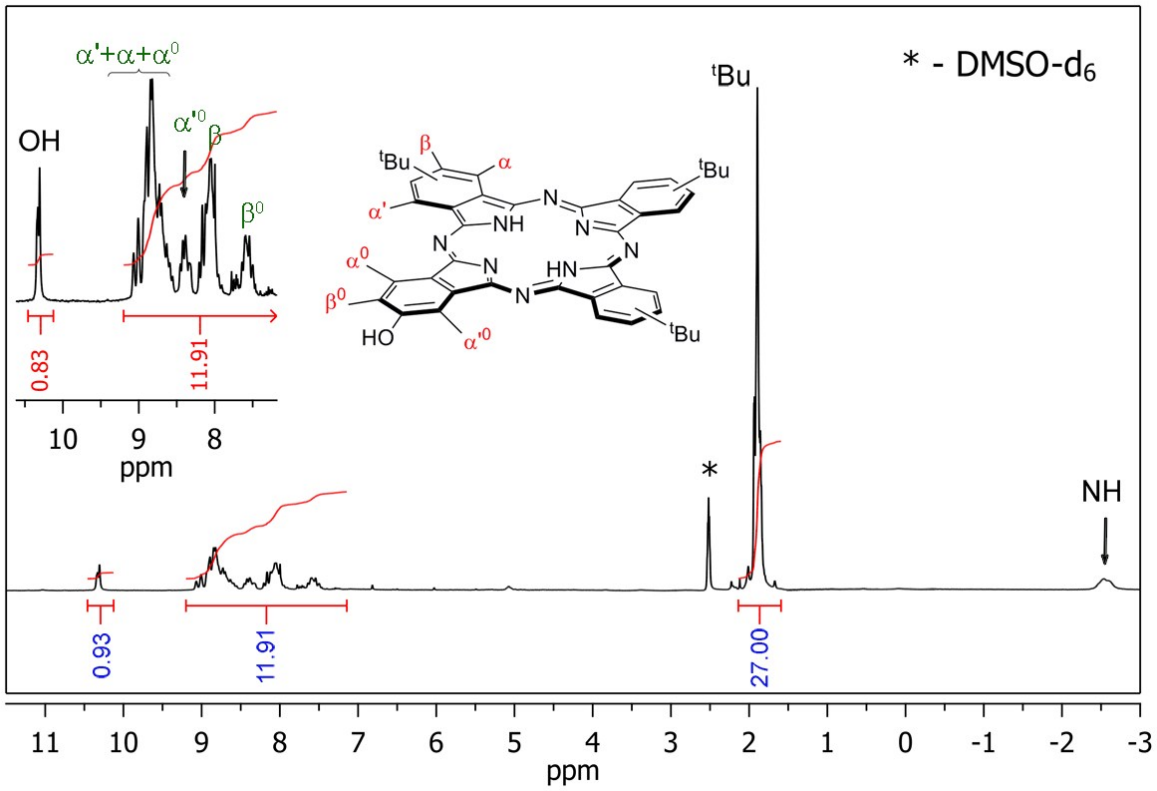

Fig. S5. ^{1}H NMR spectrum (CCl_4+5%DMSO-d_6; 298K, 200MHz) of Compound **1**.

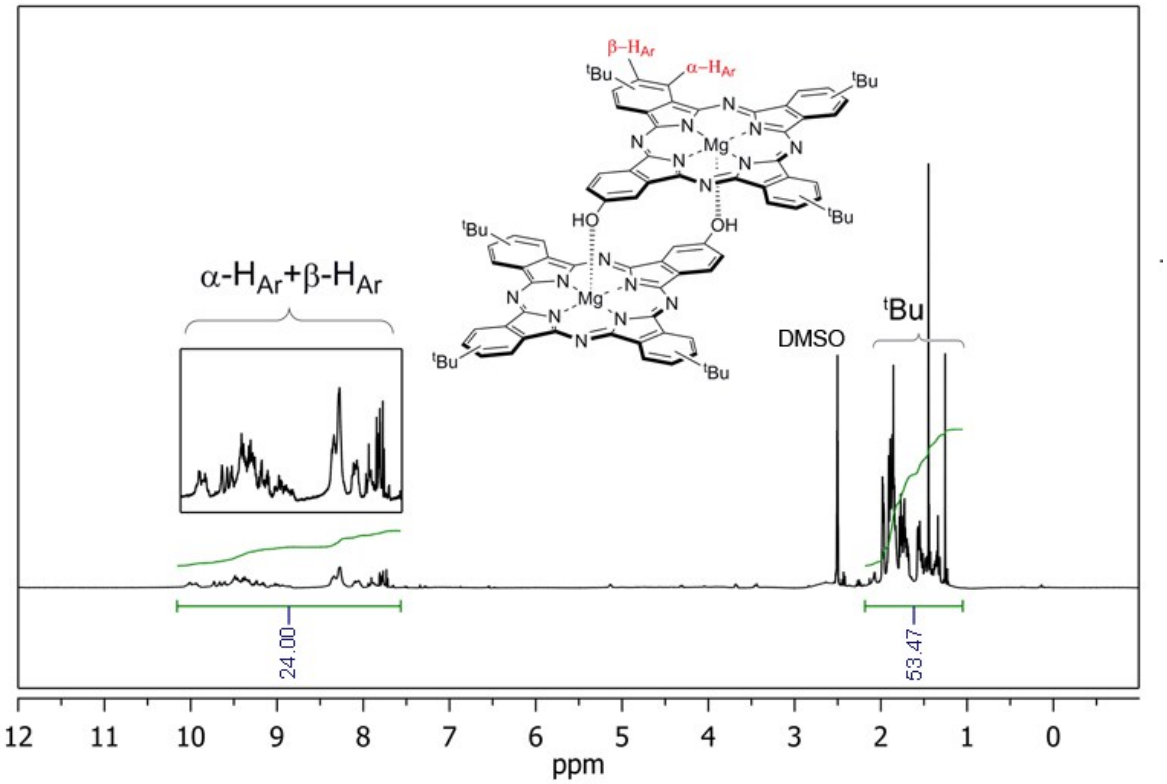

Fig. S6. ^{1}H NMR spectrum (CCl_4+5%DMSO-d_6; 333K, 500MHz) of Compound **2**.

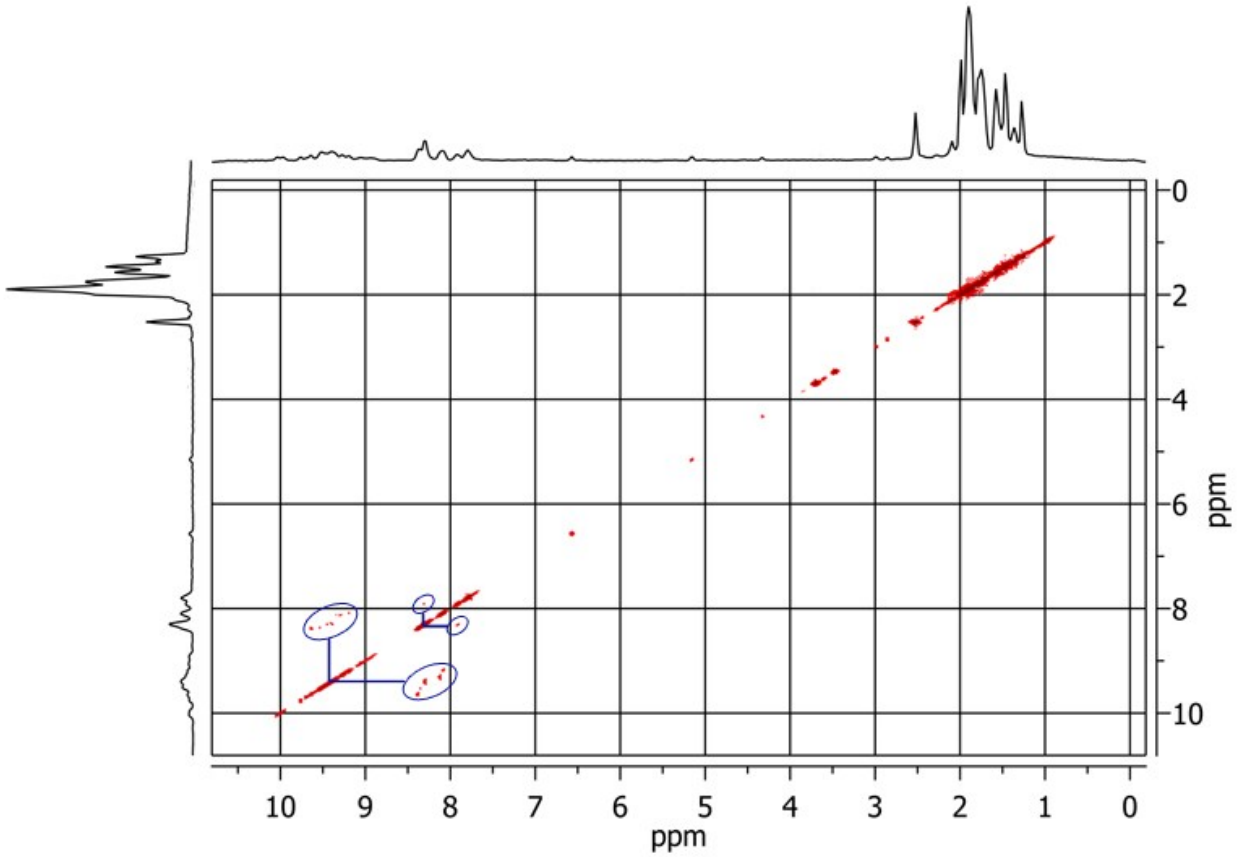

Fig. S7. $^{1}H–^{1}H$ COSY NMR spectrum (CCl_4+5%DMSO-d_6; 333K, 500MHz) of Compound **2**.

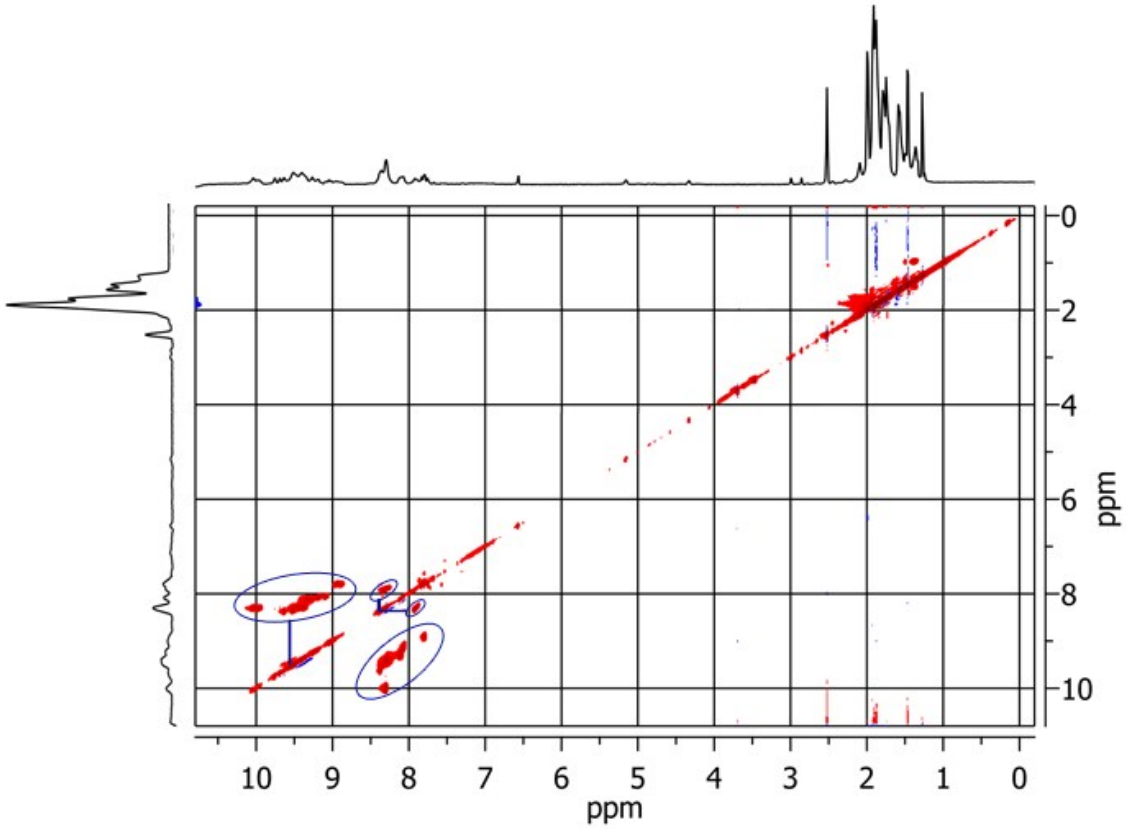

Fig. S8. $^{1}H–^{1}H$ TOCSY NMR spectrum (CCl_4+5%DMSO-d_6; 333K, 500MHz) of Compound **2**.

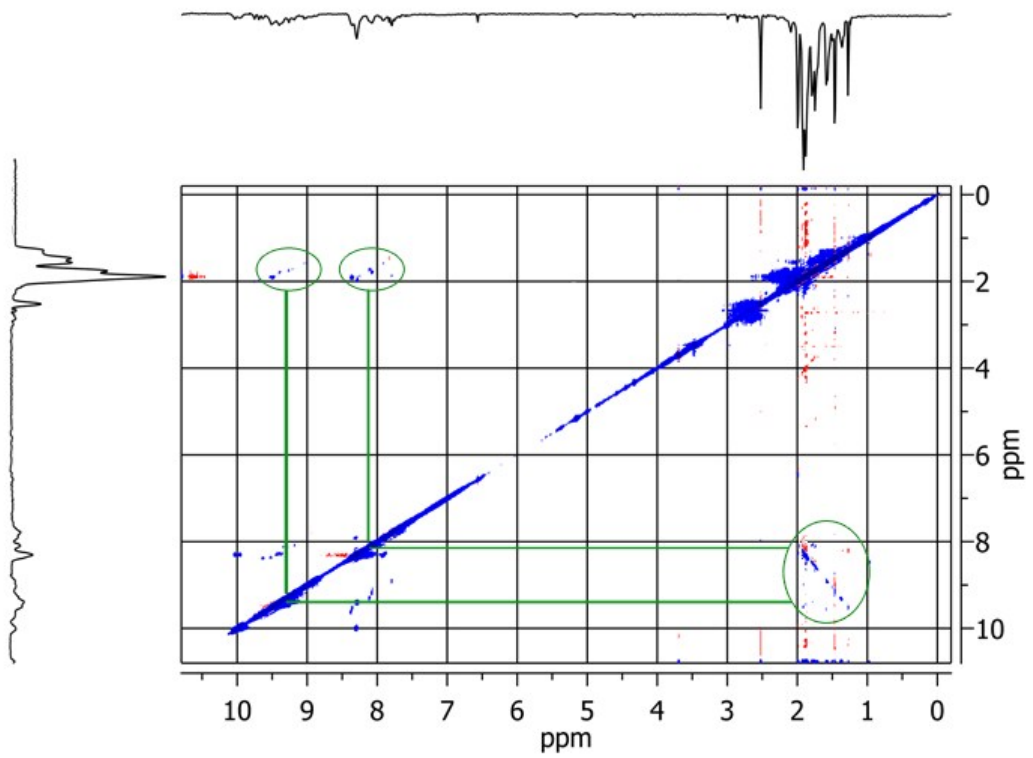

Fig. S9. $^{1}H–^{1}H$ NOESY NMR spectrum (CCl_4+5%DMSO-d_6; 333K, 500MHz) of Compound **2**.

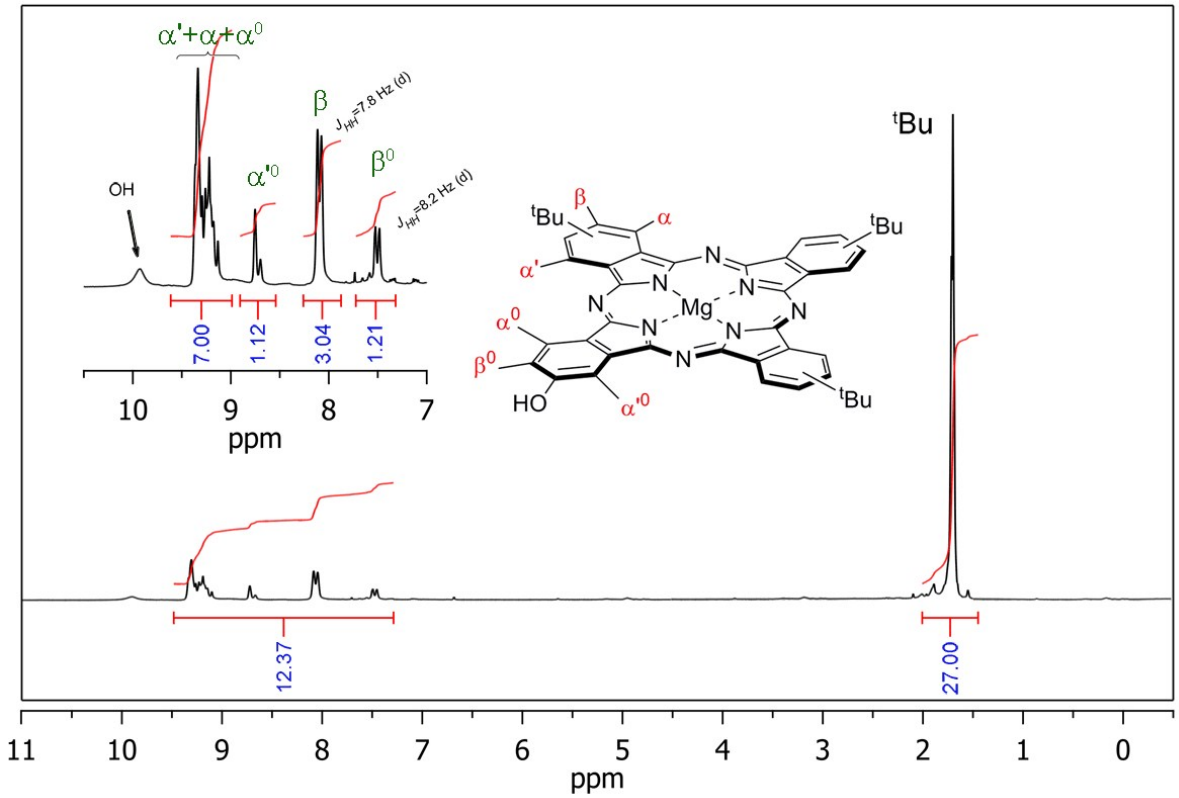

Fig. S10. ^{1}H NMR spectrum (CCl_4; 298K, 200MHz) of Compound **3**.

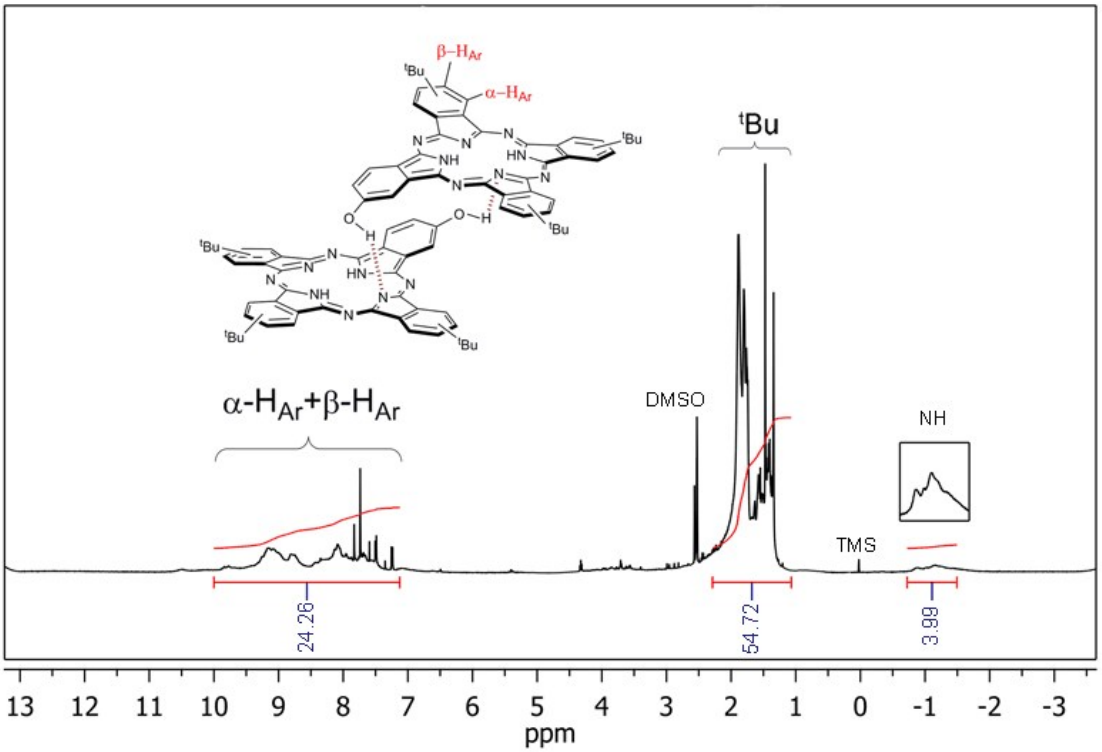

Fig. S11. ^{1}H NMR spectrum (CCl_4+5%DMSO-d_6; 333K, 500MHz) of Compound **4**.

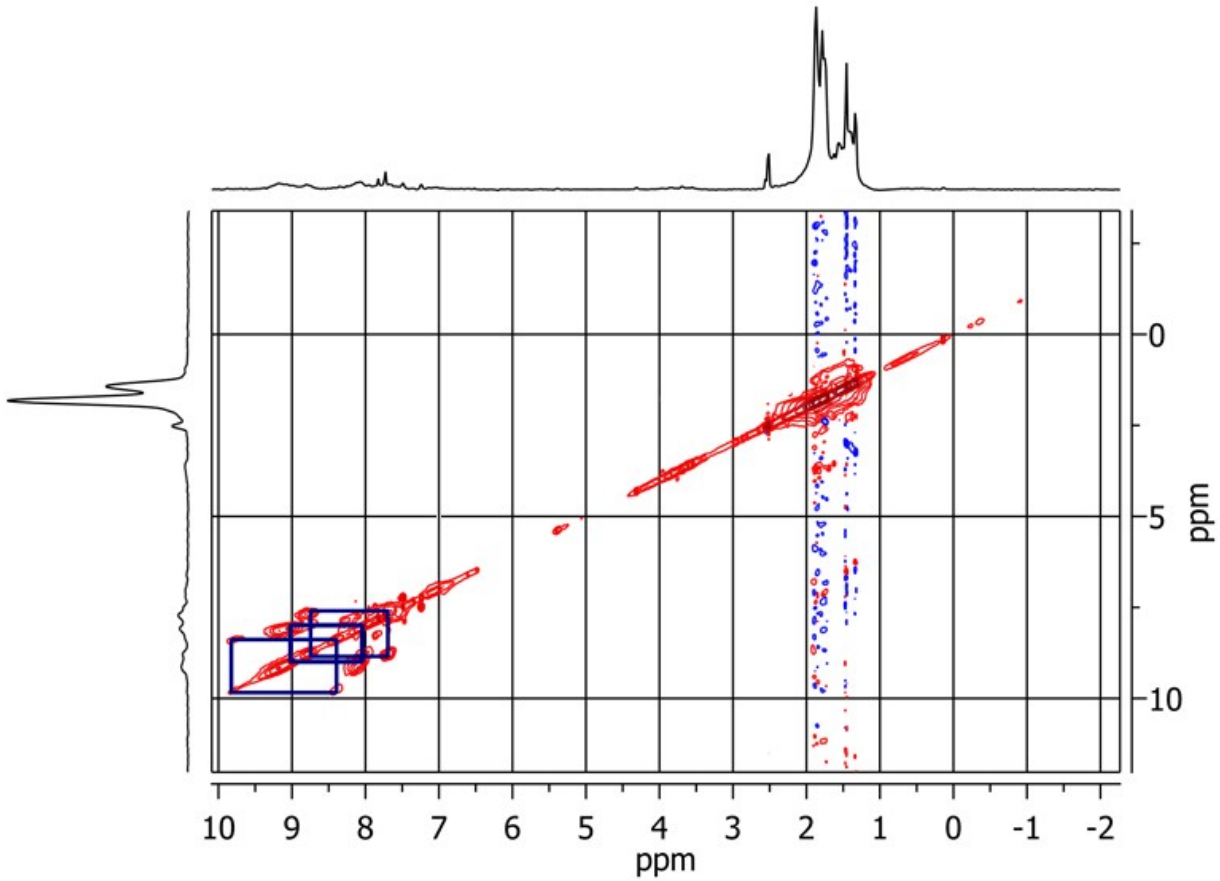

Fig. S12. ^{1}H–^{1}H TOCSY NMR spectrum (CCl_4+5%DMSO-d_6; 333K, 500MHz) of Compound **4**.

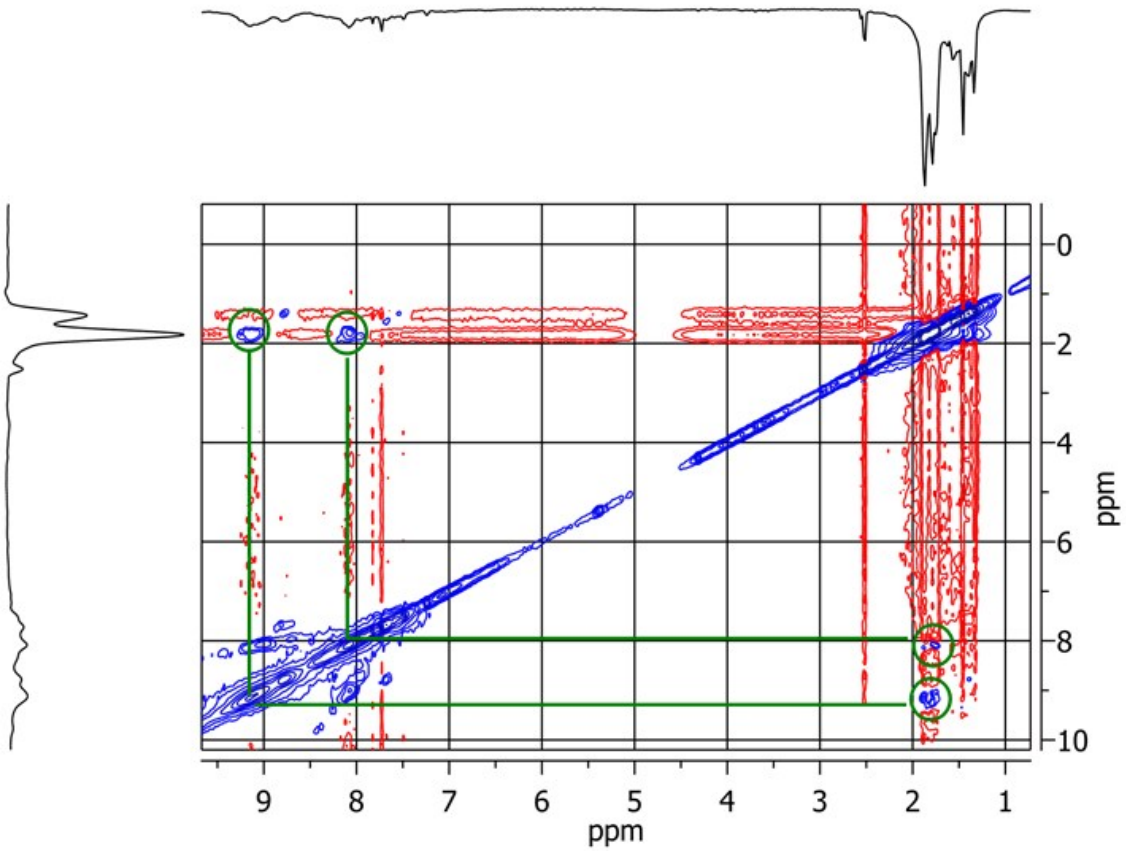

Fig. S13. $^{1}H–^{1}H$ NOESY NMR spectrum (CCl_4+5%DMSO-d_6; 333K, 500MHz) of Compound **4**.

3. FTIR spectra

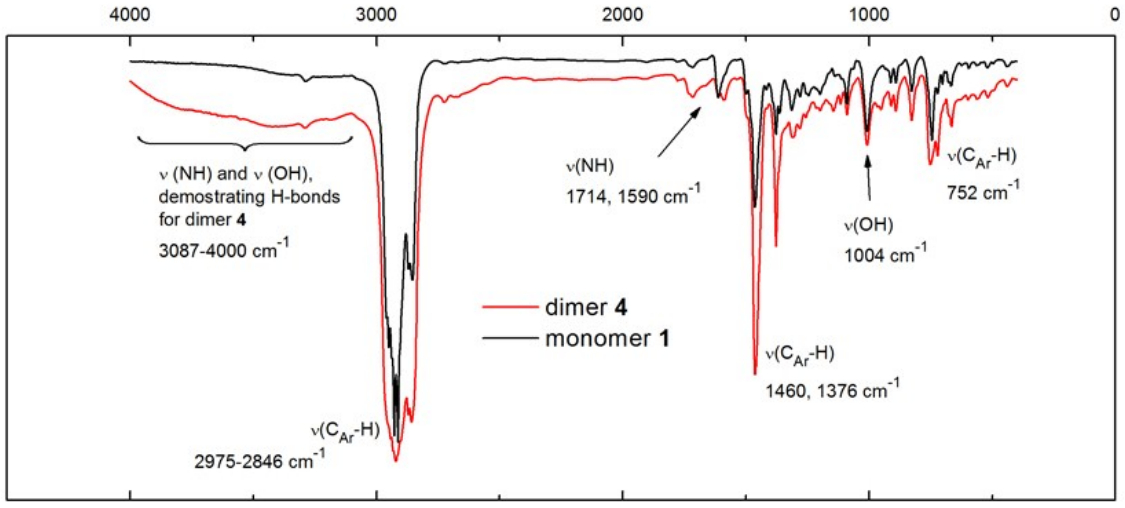

Fig. S14. FT–IR spectra (CCl_4) of Compounds **1** and **4**.

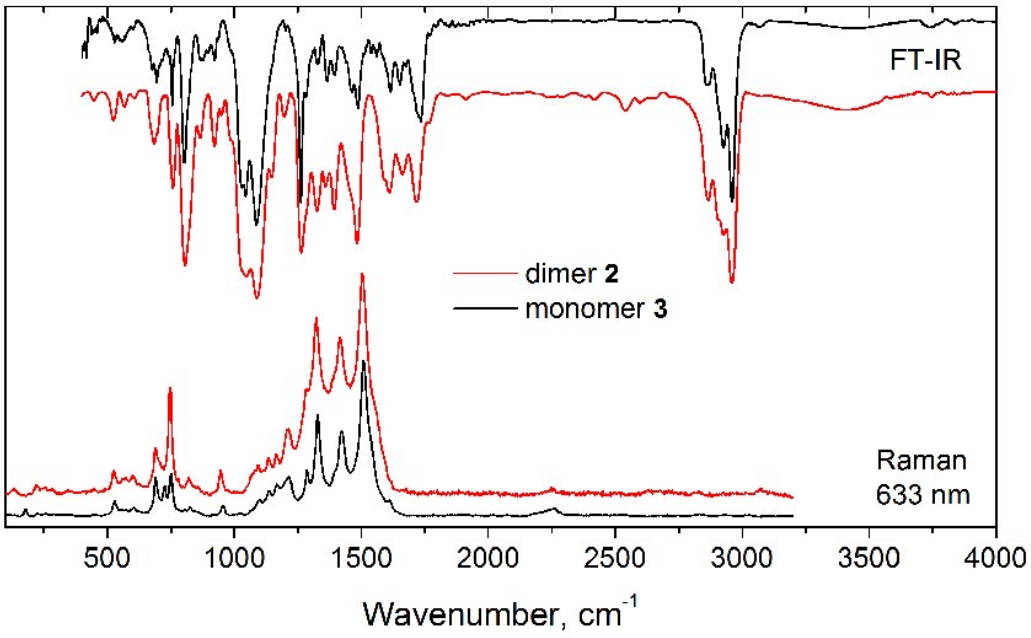

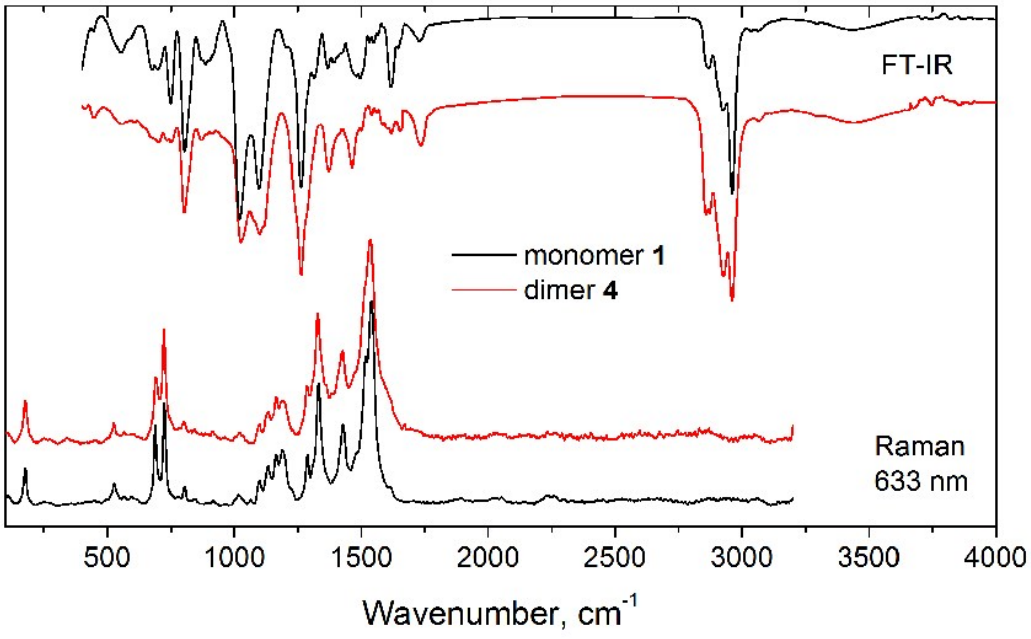

Fig. S15. FT–IR (KBr) and Raman (633 nm) spectra of Compounds **1**–**4**.

4. UV/Vis spectra

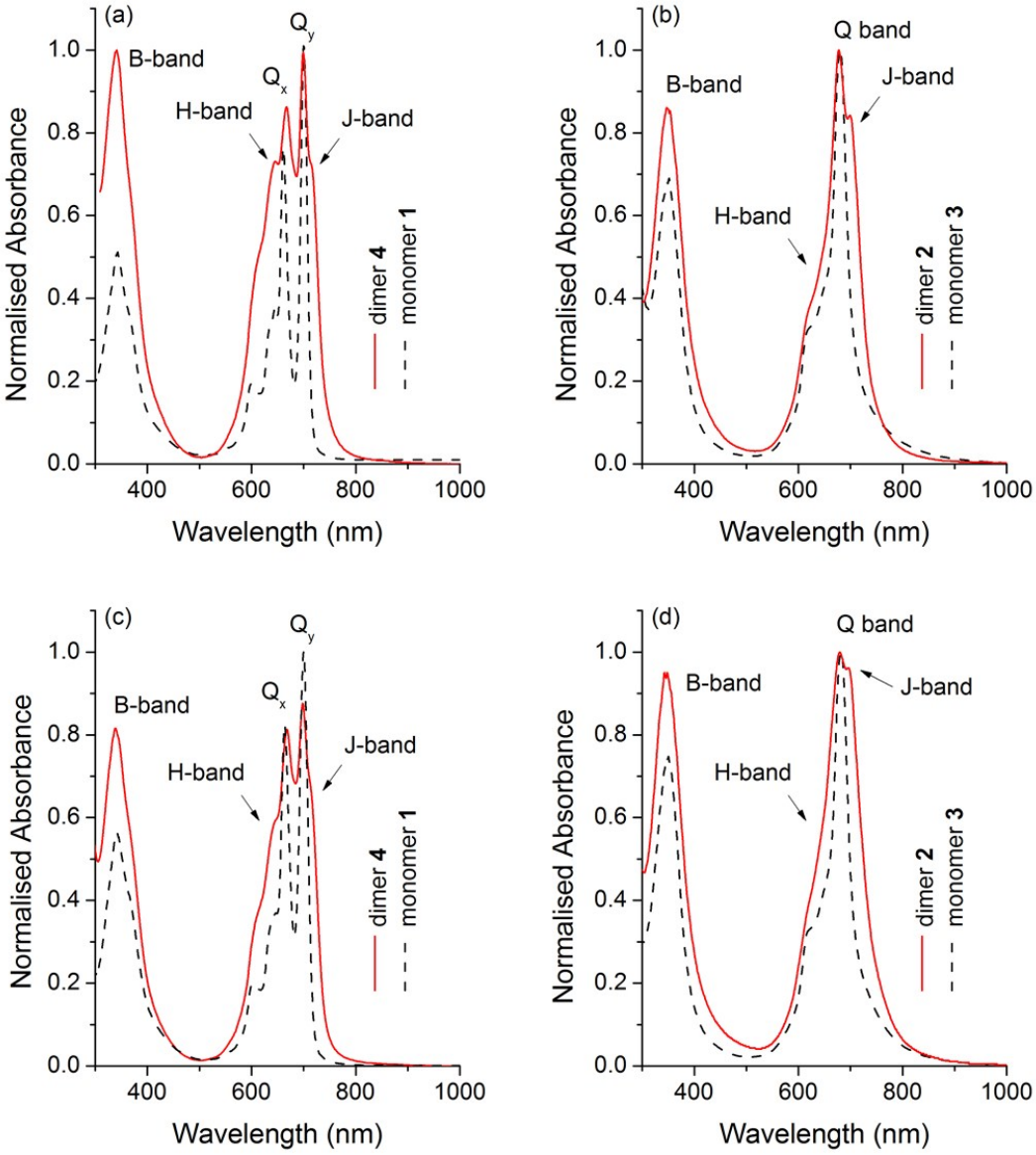

Fig. S16. Normalised UV/Vis spectra of dimers **2,4** and corresponding monomers **1,3** in CCl_4 (a,b) and $CHCl_3$ (c,d). Concentration of compounds was chosen to be ~1.5×10^{-6} mol·dm^3.

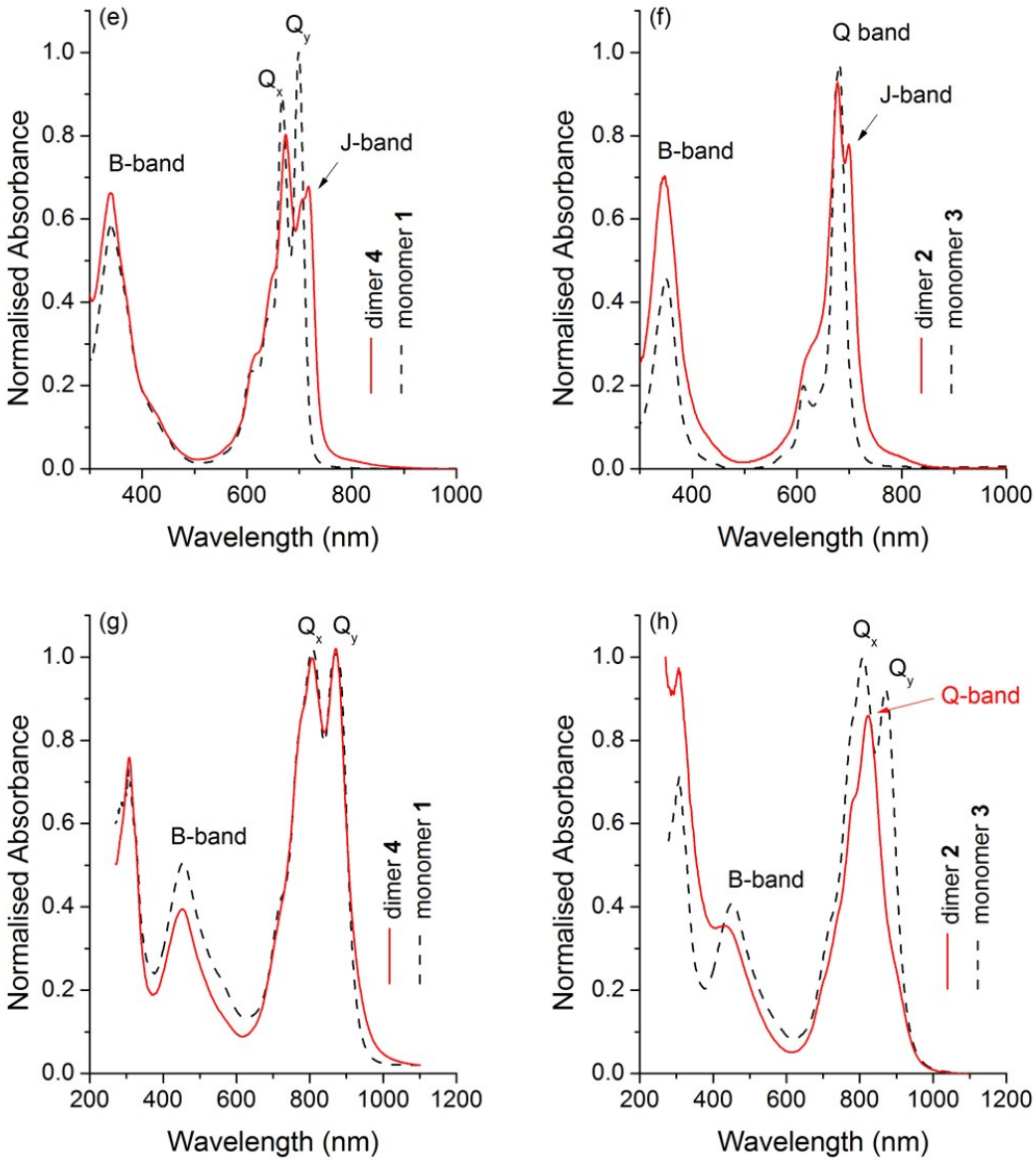

Fig. S17. Normalised UV/Vis spectra of dimers **2,4** and corresponding monomers **1,3** in DMF (a,b) and conc. H_2SO_4 (c,d). Concentration of compounds was chosen to be ~1.5×10^{-6} mol•dm^3.

As can be seen from Figs. S16 and S17, non-polar solvents contribute to the formation of H-type aggregates, with the dimers and monomers being exhibited different tendency to aggregation. Non-aggregated patterns can be obtained in THF, DMF and some other polar solvents. J-Dimers are stable in common solvents regardless molar density, with the exception of strong acids. However, exactly one of these strong acids - conc. $HClO_4$ - was chosen to transform dimer **2** to dimer **4**. In addition, magnesium dimer **2** is more stable than corresponding monomer **3** when dissolved in conc. H_2SO_4.

5. Fluorescence study

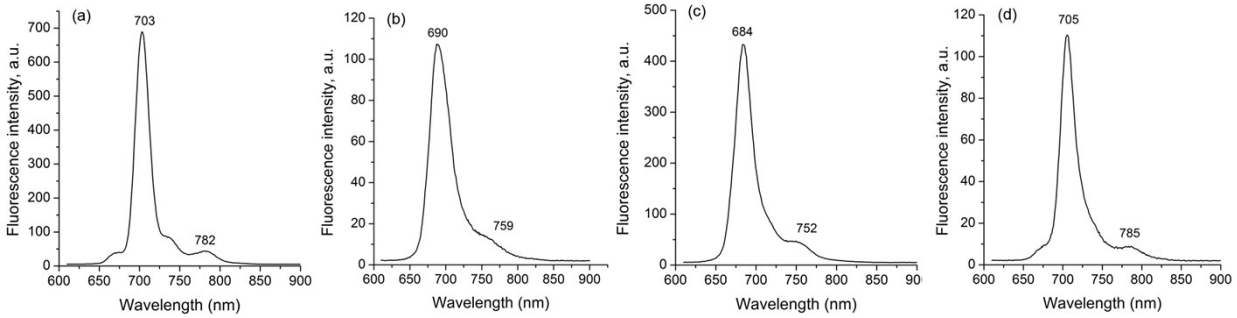

Fig. S18. Fluorescence emission (λ_{ex} = 600 nm) spectra of phthalocyanines **1** – (a), **2** – (b), **3** – (c) and **4** – (d) in THF (C=4.8×10^{-6} mol·dm^3).

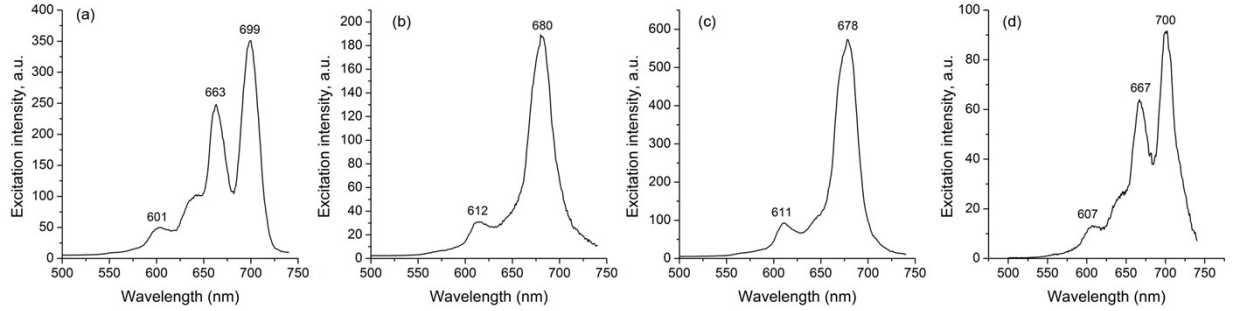

Fig. S19. Fluorescence excitation (λ_{em} = 750 nm) spectra of phthalocyanines **1** – (a), **2** – (b), **3** – (c) and **4** – (d) in THF (C=4.8×10^{-6} mol·dm^3).

It is important to note the similarity of the excitation spectra of dimeric phthalocyanine **2** and **4** with the corresponding monomers **1** and **3**, respectively. This result is due to a shifting of the macrocycles upon excitation, resulting in a partial loss of the stabilising forces – coordination bonds Mg···O in **2** and hydrogen bonds in ligand **4**. This reduces the intermolecular π-π- interactions of the macrocycles similar to zinc J-dimer in pyridine [1], and dimeric molecules exhibit properties of the monomers, but only on excitation, because their UV/Vis spectra demonstrate significant differences from the corresponding monomers. Distortion of the macrocycles in dimeric structures, which can be enhanced on excitation, leads to a redistribution of the energy, both within and between the macrocycles, and results in partial quenching of the fluorescence and a decrease in the fluorescence quantum yield (Φ_F = 0.01), in comparison with the corresponding monomers (Φ_F = 0.05).

6. Thermoanalytical study

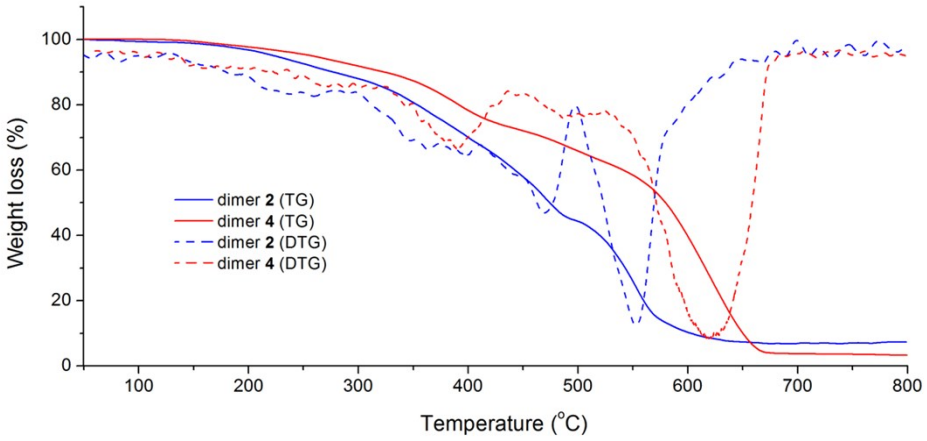

Fig. S20. TG and DTG curves of dimeric phthalocyanines **2** and **4**.

7. DFT Calculations

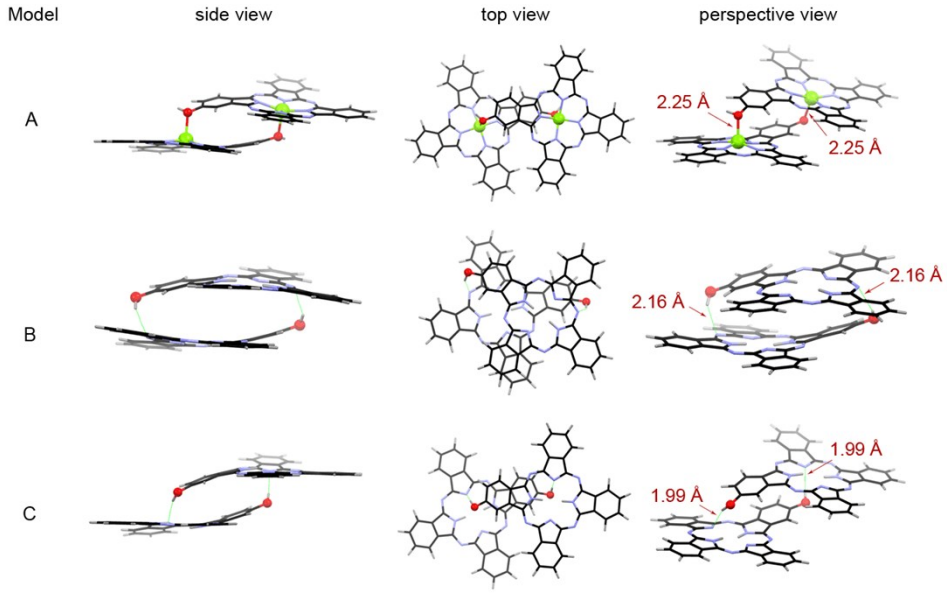

Fig S21. DFT-optimised structures of models based on compounds **2,4**. *Tert*-butyl groups were replaced with hydrogen atoms for clarity.

Table S1. General computed data for the Models based on dimeric complexes **2,4**. [a]

Property	Model		
	A	B	C
Total energy, a.u.	-3884.0197	-3483.8718	-3483.8734
Symmetry point group	C_2	C_2	C_2
Type of the dimer	*J*	*H*	*J*
Dipole moment (μ), Debye	2.18	1.50	1.25
$E_g = [E_{LUMO}–E_{HOMO}]$, eV	1.38	1.34	1.32
The angle of slippage, deg.	20.4	59.8	25.3
The tilt angle, deg.	16.7	9.1	4.5
The relative rotation of the macrocycles, deg.	131.9	121.1	134.25
The distance between the centroid of one macrocycle and $4N_{iso}$ plane of the second one, Å	3.82	4.00	4.34
The distortion of isoindoline fragment bearing OH group, deg.	15.7	17.1	21.6
The distance between the central metal ion of the first macrocycle and O atom of the OH group of the second one, Å	2.25	–	–
The H-bond length between the N atom of the first macrocycle and H atom of the OH group of the second one, Å	–	2.16	1.99

[a] according to DFT calculations (PBE/cc-pVDZ).

Table S2. Second order perturbation theory analysis of Fock matrix in NBO basis for Models A-C[a].

Model	Donor	Acceptor	Stabilization energy, E(2), kcal/mol
	Bonds Mg ··· O		
A	[46] CR (O42)	[286] LV (Mg99)	0.35
	[102] LP_1 (O42)	[286] LV (Mg99)	11.11
	[103] LP_2 (O42)	[286] LV (Mg99)	28.07
	[92] CR (O100)	[285] LV (Mg41)	0.35
	[113] LP_1 (O100)	[285] LV (Mg41)	11.11
	[114] LP_2 (O100)	[285] LV (Mg41)	28.13
	Bonds O–H ··· N		
B	[100] LP (N95)	[361] BD* (O41–H57)	5.62
	[89] LP (N38)	[446] BD* (O98–H114)	5.59
C	[96] LP_1 (N83)	[360] BD* (O41–H57)	11.30
	[86] LP_1 (N26)	[446] BD* (O98–H114)	11.25

[a] Structures of Models A-C are presented in Fig. S13. The numbers of pre-orthogonal NBOs are indicated in square brackets. Notations: 'LP' - lone pair; 'CR' - single-center; 'LV' - lone vacant orbitals. Calculations were fulfilled on Gamess-US package (DFT//CAM-B3LYP/cc-pVDZ) with NBO 6.0 module being integrated.

8. References

1. A.Yu. Tolbin, V.E. Pushkarev, I.O. Balashova, A.V. Dzuban, P.A. Tarakanov, S.A. Trashin, L.G. Tomilova, N.S. Zefirov, *New J. Chem.*, 2014, **38**, 5825-5831.